NACA RM L57G11a

NACA

RESEARCH MEMORANDUM

THEORETICAL DETERMINATION OF LOW-DRAG SUPERCAVITATING HYDROFOILS AND THEIR TWO-DIMENSIONAL CHARACTERISTICS AT ZERO CAVITATION NUMBER

By Virgil E. Johnson, Jr.

Langley Aeronautical Laboratory
Langley Field, Va.

NATIONAL ADVISORY COMMITTEE
FOR AERONAUTICS

WASHINGTON

September 30, 1957
Declassified May 16, 1958

NACA RM L57G11a

NATIONAL ADVISORY COMMITTEE FOR AERONAUTICS

RESEARCH MEMORANDUM

THEORETICAL DETERMINATION OF LOW-DRAG SUPERCAVITATING HYDROFOILS AND THEIR TWO-DIMENSIONAL CHARACTERISTICS AT ZERO CAVITATION NUMBER

By Virgil E. Johnson, Jr.

SUMMARY

The linearized theory of Tulin and Burkart for two-dimensional supercavitating hydrofoils operating at zero cavitation number is applied to the derivation of two new low-drag configurations. These sections were derived by assuming additional terms in the vorticity distribution of the equivalent airfoil; in particular, three and five terms were considered. The characteristics of both the three- and five-term airfoils are shown to be superior to the Tulin-Burkart configuration. For example, the two-dimensional lift-drag ratios of these new sections operating at their design lift coefficient are theoretically about 45 percent and 80 percent greater than the Tulin-Burkart configuration.

A simplified calculation of the location of the cavity boundary streamline for arbitrary configurations is also presented. The method assumes that the contribution of camber to the equivalent airfoil vorticity distribution is concentrated at the center of pressure.

INTRODUCTION

In reference 1 Tulin and Burkart present a linearized theory for determining the characteristics of supercavitating two-dimensional hydrofoils of arbitrary section operating at zero cavitation number. It is shown that the hydrofoil problem may be transformed into an equivalent airfoil problem which can be treated by well-known thin-airfoil theory. The theory shows that hydrofoils with high lift-drag ratios are those whose equivalent airfoils have their centers of pressure as far aft as possible while maintaining all positive vorticity over the chord. In reference 1 such a low-drag section was chosen by specifying only two sine terms in the pressure-distribution expansion (or equivalently, the vorticity distribution) and then these two coefficients were adjusted so that the necessary conditions for high lift-drag ratios were satisfied.

The purpose of the present report is to derive hydrofoils whose airfoil center of pressure is further aft than the Tulin-Burkart configuration and thus even higher lift-drag ratios are obtained. One obvious means of accomplishing this is to specify a given pressure distribution on the airfoil and then to determine the Fourier coefficients which describe it. This procedure usually will not lead to a closed-form expression for the airfoil or hydrofoil shape; however, the method does permit adequate solutions in tabular form to be made. In the present case, it was reasoned that superior configurations could be derived merely by choosing more terms in the vorticity series expansion and adjusting the coefficients for maximum lift-drag ratio exactly as was done by Tulin and Burkart. In this manner, the results would be in a closed form. The number of terms chosen for the analysis was specified as three for the first case and five for the second case. The results of calculations based on these presumptions are presented.

Since, for practical reasons the hydrofoils must have some thickness; the shape of the cavity streamline leaving the leading edge is required. The thickness of the hydrofoil that can be permitted is then such that the hydrofoil upper surface lies below this free streamline. The linearized theory permits, in principle, this streamline location to be calculated; however, when the expression for the airfoil vorticity distribution becomes very lengthy, the calculation is very difficult. If the vorticity due to camber is assumed to be concentrated at the center of pressure of the airfoil, the problem is greatly simplified. The results of an analysis based on this assumption are also presented.

SYMBOLS

A_n coefficients of sine-series expansion of airfoil vorticity distribution; that is,

$$\Omega(\bar{x}) = 2V\left(A_0 \cot \frac{\theta}{2} + A_1 \sin \theta + A_2 \sin 2\theta \ . \ . \ . \ A_n \sin n\theta\right)$$

A_0' value of A_0 when $\alpha = 0$; that is, $A_0' = -\frac{1}{\pi}\int_0^{\pi} \frac{d\bar{y}}{d\bar{x}}\, d\theta$

a distance from airfoil leading edge to center of pressure in chords

$$a_2 = -\frac{A_2}{A_1}$$

$$a_3 = \frac{A_3}{A_1}$$

c	chord
C_D	drag coefficient, D/qc
C_L	lift coefficient, L/qc
$C_{L,d}$	design lift coefficient at $\alpha = 0$
C_m	pitching-moment coefficient about leading edge, M/qc^2
$C_{m,3}$	third-moment coefficient about leading edge, M_3/qc^4
C_p	pressure coefficient, $\frac{p - p_\infty}{q}$
D	drag force
k	number of terms in summation $\sum_{n=1}^{k} A_n \sin n\theta$
L	lift force
M	pitching moment about leading edge
M_3	third moment about leading edge, $2\int_0^{\bar{c}} p(\bar{x})\bar{x}^3 d\bar{x}$
p	local pressure
p_∞	ambient or free-stream pressure
q	dynamic pressure, $\frac{1}{2}\rho V^2$
l	distance from section reference line to upper cavity streamline
V	speed of advance, fps
u	perturbation velocity in x-direction
v	perturbation velocity in y-direction

x' dimensionless distance parameter along X-axis, x/c

x distance along X-axis

y' dimensionless distance parameter along Y-axis, y/c

y distance along Y-axis

α geometric angle of attack, radians

Γ circulation

Ω vorticity

θ variable related to distance along equivalent airfoil chord by equation $\bar{x} = \frac{1}{2}\bar{c}(1 - \cos\theta)$

Subscripts:

α due to A_0 or if $A_0' = 0$ is due to angle of attack

c due to camber

Barred symbols refer to quantities in the airfoil plane and unbarred symbols to quantities in the hydrofoil plane.

SUMMARY OF THE TULIN-BURKART LINEARIZED THEORY

Since it will be necessary in the derivation of the new hydrofoils to refer frequently to the linear theory of reference 1, a summary of the principal results of that theory is useful.

In reference 1 it is shown that the problem of a hydrofoil operating at zero cavitation number in the Z-plane may be transformed into an airfoil problem in the $\bar{Z}$-plane by the relationship $\bar{Z} = -\sqrt{Z}$. By denoting properties of the equivalent airfoil with barred symbols and those of the hydrofoil with unbarred symbols, the following relationships are derived:

$$\frac{d\bar{y}}{d\bar{x}}(\bar{x}) = \frac{dy}{dx}\left(\bar{x}^2\right) \tag{1}$$

$$\bar{u}(\bar{x}) = u\left(\bar{x}^2\right) \tag{2}$$

$$C_L = \bar{C}_m = \frac{\pi}{2}\left(A_o + A_1 - \frac{A_2}{2}\right) \tag{3}$$

$$C_D = \frac{1}{8\pi}\left(\bar{C}_L{}^2\right) = \frac{\pi}{2}\left(A_o + \frac{A_1}{2}\right)^2 \tag{4}$$

$$C_m = \bar{C}_{m,3} = \frac{\pi}{32}\left(5A_o + 7A_1 - 7A_2 + 3A_3 - \frac{A_4}{2}\right) \tag{5}$$

The coefficients A_n are the thin-airfoil coefficients in the sine-series expansion of the velocity perturbations $\bar{u}(\bar{x})$ where

$$\bar{u}(\bar{x}) = V\left(A_o \cot\frac{\theta}{2} + \sum_{n=1}^{\infty} A_n \sin n\theta\right) \tag{6}$$

where

$$\bar{x} = \frac{1}{2}\bar{c}(1 - \cos\theta) \qquad (0 \leqq \theta \leqq \pi) \tag{7}$$

Since $\bar{u}(\bar{x}) = 2\Omega(\bar{x})$, equation (6) defines the vorticity distribution on the equivalent airfoil as

$$\Omega(\bar{x}) = 2V\left(A_o \cot\frac{\theta}{2} + \sum_{n=1}^{\infty} A_n \sin n\theta\right) \tag{8}$$

The values of the A coefficients can be found for a given configuration from the following equations:

$$A_o = -\frac{1}{\pi}\int_0^{\pi} \frac{d\bar{y}}{d\bar{x}}\, d\theta + \alpha = \alpha + A_o' \tag{9a}$$

$$A_n = \frac{2}{\pi}\int_0^{\pi} \frac{d\bar{y}}{d\bar{x}} \cos n\theta\, d\theta \tag{9b}$$

The first term in equation (8); that is, the A_0 term, is the vorticity due to angle of attack and the second term is that due to camber. In order to isolate the effects of camber, A_0 will be considered zero. Any section profile derived on this basis will also, for convenience, be oriented with respect to the $\bar{X}$-axis in such a manner that $A_0' = 0$. From equation (9a) these conditions require that α also be equal to zero. Thus, the derived orientation is defined as the zero-angle-of-attack case.

When A_0 is set equal to zero, the hydrofoil lift-drag ratio for a given lift coefficient is obtained from equations (3) and (4) as follows:

$$\frac{C_L}{C_D} = \frac{\left(A_1 - \frac{A_2}{2}\right)^2}{A_1^2/4} \frac{\pi}{2C_L} = 4\left(1 - \frac{1}{2}\frac{A_2}{A_1}\right)^2 \tag{10}$$

Obviously, for maximum lift-drag ratio, $-\frac{A_2}{A_1}$ must be as large as possible. However, if the assumed condition that a cavity exists only on the upper surface is to be real, the vorticity distribution given by equation (8) must be positive in the interval $0 \leqq \theta \leqq \pi$; that is, the pressure on the hydrofoil lower surface must be positive over the entire chord, otherwise a cavity will exist on the lower surface. Thus, for maximum hydrofoil lift-drag ratio, $-\frac{A_2}{A_1}$ must be as large as possible and still satisfy the condition that

$$\Omega(\bar{x}) = 2V \sum_{n=1}^{\infty} A_n \sin n\theta \geqq 0 \qquad (0 \leqq \theta \leqq \pi) \tag{11}$$

With the stipulation that the vorticity distribution is defined by only two terms in equation (11), reference 1 finds the optimum relationship between A_1 and A_2 as $-\frac{A_2}{A_1} = \frac{1}{2}$. This results in a hydrofoil configuration given by the equation

$$\frac{y}{c} = \frac{A_1}{2}\left[\frac{x}{c} + \frac{8}{3}\left(\frac{x}{c}\right)^{3/2} - 4\left(\frac{x}{c}\right)^2\right] \tag{12}$$

From equation (3) the design lift coefficient (that is, for $\alpha = 0$) for this section is

$$C_{L,d} = \frac{5\pi A_1}{8} \tag{13}$$

and the lift-drag ratio for this condition as obtained from equation (10) is

$$\frac{L}{D} = \frac{25}{4}\left(\frac{\pi}{2C_L}\right) \tag{14}$$

Since $\pi/2C_L$ represents the lift-drag ratio of a flat plate, the configuration given by equation (12) has a lift-drag ratio 25/4 times as great as that of the flat plate. When the hydrofoil given in equation (12) is operated at an angle of attack, the lift-drag ratio becomes

$$\frac{L}{D} = \frac{\alpha + \frac{2}{\pi} C_{L,d}}{\left(\alpha + \frac{4}{5\pi} C_{L,d}\right)^2} \tag{15}$$

The present analysis is concerned with the derivation of two new configurations. The problem is exactly the same as that discussed in reference 1 and summarized above except that the vorticity distribution given by equation (11) is defined by: (1) three terms and (2) five terms.

DERIVATION OF LOW-DRAG HYDROFOILS AND THEIR CHARACTERISTICS

Statement of Problem

The problem under consideration is (1) to find the values of the coefficients in the vorticity equation

$$\Omega(\bar{x}) = 2V \sum_{n=1}^{k} A_n \sin n\theta \geqq 0 \qquad \left(0 \leqq \theta \leqq \pi\right) \tag{16}$$

such that $-\frac{A_2}{A_1}$ is a maximum for the specific cases of $k = 3$ and $k = 5$, and (2) to use the method of reference 1 to find the shape of

the hydrofoil which when transformed to the airfoil plane has the vorticity distribution given in equation (16).

Three-Term Solution (k = 3)

For the case $k = 3$, the vorticity distribution given in equation (16) becomes

$$\Omega(\bar{x}) = 2V\left(A_1 \sin\theta + A_2 \sin 2\theta + A_3 \sin 3\theta\right) \geqq 0 \tag{17}$$

The solution of equation (17) is obtained in the following manner. Let

$$a_2 = -\frac{A_2}{A_1} \tag{18}$$

$$a_3 = \frac{A_3}{A_1} \tag{19}$$

The problem is now to find a_2 and a_3 so that a_2 is a maximum and

$$\sin\theta - a_2 \sin 2\theta + a_3 \sin 3\theta \geqq 0 \qquad \left(0 \leqq \theta \leqq \pi\right) \tag{20}$$

Substituting trigonometric identities for the functions of the multiples of θ, equation (20) may be written as

$$1 - 2a_2 \cos\theta + 3a_3 - 4a_3 \sin^2\theta \geqq 0 \tag{21}$$

The minimum of equation (21) occurs when

$$\theta = \cos^{-1}\frac{a_2}{4a_3}$$

Substituting this value of θ into equation (21) gives

$$1 - \frac{2{a_2}^2}{4a_3} + 3a_3 - 4a_3\left(1 - \frac{{a_2}^2}{16{a_3}^2}\right) \geqq 0 \tag{22}$$

or

$$4a_3 - 4a_3^2 - a_2^2 \geq 0 = b \qquad (b \geq 0) \quad (23)$$

Therefore,

$$a_2 = \pm\sqrt{4a_3 - 4a_3^2 - b} \quad (24)$$

and the term under the radical has a maximum at $a_3 = \frac{1}{2}$. Thus,

$$a_2 = \pm\sqrt{1 - b} \quad (25)$$

and the maximum possible value of a_2 is 1 which occurs when $b = 0$ and $a_3 = \frac{1}{2}$. Since these values are obtained by considering the minimum value of the vorticity or pressure on the airfoil, the condition $\Omega(\bar{x}) \geq 0$ is satisfied for all values of θ $(0 \leq \theta \leq \pi)$. Thus the solution for the vorticity distribution for the case $k = 3$ is

$$\Omega(\bar{x}) = 2VA_1\left(\sin\theta - \sin 2\theta + \frac{1}{2}\sin 3\theta\right) \quad (26)$$

The airfoil slope which has the vorticity distribution given by equation (26) is obtained from reference 2 and is given as follows:

$$\frac{d\bar{y}}{d\bar{x}} = A_1\left(\cos\theta - \cos 2\theta + \frac{1}{2}\cos 3\theta\right) \quad (27)$$

Substituting trigonometric identities for the functions of the multiples of θ, equation (27) becomes

$$\frac{d\bar{y}}{d\bar{x}} = A_1\left(2\cos^3\theta - 2\cos^2\theta - \frac{1}{2}\cos\theta + 1\right) \quad (28)$$

and since $\cos\theta = 1 - 2\frac{\bar{x}}{\bar{c}}$

$$\frac{d\bar{y}}{d\bar{x}}(\bar{x}) = A_1\left[2\left(1 - 2\frac{\bar{x}}{\bar{c}}\right)^3 - 2\left(1 - 2\frac{\bar{x}}{\bar{c}}\right)^2 - \frac{1}{2}\left(1 - 2\frac{\bar{x}}{\bar{c}}\right) + 1\right] \tag{29}$$

The slope of the equivalent hydrofoil is obtained from reference 1 and is given as follows:

$$\frac{dy}{dx}(x) = \frac{d\bar{y}}{d\bar{x}}\left(\sqrt{x}\right) \tag{30}$$

Equation (30) states that the slope of the hydrofoil can be obtained from equation (29) by replacing $\bar{x}$ with $\sqrt{x}$.

Thus, since $\bar{c} = \sqrt{c}$,

$$\frac{dy}{dx} = A_1\left[2\left(1 - 2\sqrt{\frac{x}{c}}\right)^3 - 2\left(1 - 2\sqrt{\frac{x}{c}}\right)^2 - \frac{1}{2}\left(1 - 2\sqrt{\frac{x}{c}}\right) + 1\right] \tag{31}$$

Integrating from 0 to x and dividing both sides by c gives the desired nondimensional hydrofoil shape; that is,

$$\frac{y}{c} = \frac{A_1}{10}\left[5\left(\frac{x}{c}\right) - 20\left(\frac{x}{c}\right)^{3/2} + 80\left(\frac{x}{c}\right)^2 - 64\left(\frac{x}{c}\right)^{5/2}\right] \tag{32}$$

By using equation (3), the lift coefficient of this hydrofoil becomes

$$C_L = \frac{\pi}{2}\left(\alpha + \frac{3A_1}{2}\right) \tag{33}$$

or for $\alpha = 0$ the design lift coefficient is

$$C_{L,d} = \frac{3\pi A_1}{4} \tag{34}$$

The following drag coefficient may be obtained by using equation (4):

$$C_D = \frac{\pi}{2}\left(\alpha + \frac{A_1}{2}\right)^2 = \frac{\pi}{2}\left(\alpha + \frac{2C_{L,d}}{3\pi}\right)^2 \tag{35}$$

For $\alpha = 0$, the lift-drag ratio is

$$\frac{L}{D} = 9\left(\frac{\pi}{2C_L}\right) \tag{36}$$

This value is nine times as large as that for a flat plate and 1.44 times as large as the value for the hydrofoil of reference 1 where $\frac{L}{D} = \frac{25}{4}\left(\frac{\pi}{2C_L}\right)$.

The following lift-drag ratio may be obtained for finite angles of attack (eqs. (32) and (34)):

$$\frac{L}{D} = \frac{\alpha + \frac{2}{\pi} C_{L,d}}{\left(\alpha + \frac{2C_{L,d}}{3\pi}\right)^2} \tag{37}$$

Five-Term Solution (k = 5)

For the case $k = 5$ the problem is to find the coefficients in the following equation:

$$\Omega(\bar{x}) = 2V\left(A_1 \sin\theta + A_2 \sin 2\theta + A_3 \sin 3\theta + A_4 \sin 4\theta + A_5 \sin 5\theta\right) \tag{38}$$

so that $\Omega(\bar{x}) \geqq 0$ and $-\frac{A_2}{A_1}$ is a maximum.

First attempts at a solution were made on a Fourier synthesizer. The synthesizer is an electronic device which is capable of generating 80 harmonics of a Fourier series and recording the summation of these components over any desired interval. The amplitude and phase angle of each harmonic generator is controllable. By using only the first five components and zero phase angle, it was discovered that a solution with $-\frac{A_2}{A_1}$ roughly equal to 1.6 was apparently possible. Unfortunately the sensitivity of the equipment was not sufficient to assure positive values of the summation of components near the leading edge. However, the synthesizer result was encouraging, since it showed that apparently there was a considerable advantage to using five terms, and revealed some of the characteristics of the solution; for example, the algebraic sign and

relative magnitude of each term. The most helpful method for obtaining the best results was that used in obtaining the three-term solution. This was to find first the minimums of equation (38) in terms of the coefficients. The term $-\frac{A_2}{A_1}$ was then assigned a value and the other coefficients were determined analytically so that three of these control points (possible minimums) were zero and the values of the others were examined. By varying the value of $-\frac{A_2}{A_1}$ and the choice of control points, a solution was obtained. The method is admittedly one of trial and error and, since the process is somewhat lengthy, the details are omitted. The best solution obtained was

$$\Omega(\bar{x}) = 2VA_1\left(\sin\theta - \frac{4}{3}\sin 2\theta + \frac{4}{3}\sin 3\theta - \frac{2}{3}\sin 4\theta + \frac{1}{3}\sin 5\theta\right) \tag{39}$$

In the course of deriving the solution it was proven that the value of $-\frac{A_2}{A_1}$ must be less than $\sqrt{2}$. Since in the solution given by equation (39) the term $-\frac{A_2}{A_1}$ has a value of 4/3 (very close to the established maximum), further efforts to find a better solution were not considered worthwhile.

By following the method used for the three-term solution, the shape of the hydrofoil corresponding to equation (39) is obtained as follows:

$$\frac{y}{c} = \frac{A_1}{315}\left[210\left(\frac{x}{c}\right) - 2{,}240\left(\frac{x}{c}\right)^{3/2} + 12{,}600\left(\frac{x}{c}\right)^2 - 30{,}912\left(\frac{x}{c}\right)^{5/2} + 35{,}840\left(\frac{x}{c}\right)^3 - 15{,}360\left(\frac{x}{c}\right)^{7/2}\right] \tag{40}$$

By using equation (3), the lift coefficient of this hydrofoil may be given as

$$C_L = \frac{\pi}{2}\left(\alpha + \frac{5A_1}{3}\right) \tag{41}$$

or for $\alpha = 0$ the design lift coefficient is

$$C_{L,d} = \frac{5\pi A_1}{6} \tag{42}$$

The following drag coefficient is obtained by using equation (4):

$$C_D = \frac{\pi}{2}\left(\alpha + \frac{A_1}{2}\right)^2 = \frac{\pi}{2}\left(\alpha + \frac{3C_{L,d}}{5\pi}\right)^2 \tag{43}$$

and for $\alpha = 0$ the lift-drag ratio is

$$\frac{L}{D} = \frac{100}{9}\left(\frac{\pi}{2C_L}\right) \tag{44}$$

This lift-drag ratio is about 11 times as large as the value for a flat plate and nearly twice as efficient as the configuration of reference 1.

For finite angles of attack,

$$\frac{L}{D} = \frac{\alpha + \frac{2}{\pi} C_{L,d}}{\left(\alpha + \frac{3}{5\pi} C_{L,d}\right)^2} \tag{45}$$

Comparison of the Low-Drag Configurations

Shape.- The shapes of the two-, three-, and five-term configurations given by equations (12), (32), and (40), respectively, are compared in figure 1. It is apparent in figure 1 that the location of maximum camber moves toward the trailing edge as $-\frac{A_2}{A_1}$ is increased. This movement corresponds to moving the center of pressure of the equivalent airfoil toward the trailing edge. It is shown in reference 1 that the limiting value of $-\frac{A_2}{A_1}$ is 2 and that for this value all the lift is concentrated at the trailing edge.

An important point to note in figure 1 is the appreciable deviation of the three- and five-term hydrofoils from the X-axis. A similar deviation from the $\bar{X}$-axis exists in the airfoil plane where it was originally assumed that the vorticity was concentrated along the $\bar{X}$-axis. Evidently the assumption is not as good for the higher term hydrofoils as it is for the two-term configuration, particularly for large magnitudes of camber. As a result, the linearized theory may be less accurate in predicting the characteristics of the new hydrofoils.

Pressure distribution.- From equations (2) and (6) and the linearized Bernoulli equation, it can be shown that the pressure distribution over the hydrofoil chord for $A_0' = 0$ is

$$C_p = \frac{p - p_\infty}{q} = 2\left(\alpha \cot \frac{\theta}{2} + \sum_{n=1}^{k} A_n \sin n\theta\right) \tag{46}$$

or separating the two components into contributions of angle of attack $C_{p,\alpha}$ and camber, $C_{p,c}$ gives

$$\frac{C_{p,\alpha}}{\alpha} = 2 \cot \frac{\theta}{2} \tag{47}$$

and

$$C_{p,c} = 2A_1 \sum_{n=1}^{k} \frac{A_n}{A_1} \sin n\theta \tag{48}$$

In equations (47) and (48) the location on the hydrofoil corresponding to a given value of θ can be found from the relationship

$$\frac{x}{c} = \frac{1}{4}(1 - \cos \theta)^2$$

since $\frac{x}{c} = \left(\frac{\bar{x}}{\bar{c}}\right)^2$. The coefficient A_1 defines a particular value of the hydrofoil lift coefficient at $\alpha = 0$; that is, the design lift coefficient $C_{L,d}$ given in equations (13), (34), and (42). Therefore, with the aid of these equations, equation (48) can also be written in terms of $C_{L,d}$ as

$$\frac{C_{p,c}}{C_{L,d}} = 2 \frac{A_1}{C_{L,d}} \sum_{n=1}^{k} \frac{A_n}{A_1} \sin n\theta \tag{49}$$

Thus, the total pressure distribution on the hydrofoils can be obtained from

$$C_p = \left(\frac{C_{p,\alpha}}{\alpha}\right)\alpha + \left(\frac{C_{p,c}}{C_{L,d}}\right)C_{L,d} \tag{50}$$

Equations (47) and (49) are plotted in figure 2 for the three hydrofoils under consideration. It is apparent in figure 2(a) that the location of the maximum pressure moves aft as $-\frac{A_2}{A_1}$ is increased. It may also be seen that the adverse pressure gradient to the left of the pressure maximum also increases as $-\frac{A_2}{A_1}$ increases. Thus the five-term hydrofoil is more susceptible to boundary-layer separation than the other two. If such separation occurs, the pressure distribution shown will be considerably altered. This of course also applies to the two- and three-term solutions but to a lesser degree. Because the adverse gradient increases so rapidly with increase in $-\frac{A_2}{A_1}$, it is believed that further increases in $-\frac{A_2}{A_1}$, attained by considering more terms in the vorticity expansion, will not be practical.

The small pressure "humps" near the leading edge of the three- and five-term hydrofoils are peculiar to the solutions found but could be eliminated by proper adjustment of the coefficients. However, the existence of these humps is probably not important in a practical configuration.

Lift-drag ratio.- The lift-drag ratio and lift coefficient given by equations (15), (37), and (45) are plotted for the three low-drag hydrofoils in figure 3. The relationship $\frac{L}{D} = \frac{\pi}{2C_L}$ for a flat plate is also included. The solid lines show the lift-drag ratios of the three low-drag hydrofoils when operated at $\alpha = 0$ but for various magnitudes of camber; that is, $C_{L,d}$. The broken curves are for the particular magnitude of camber for which $C_{L,d} = 0.2$ and 0.4, but the angle of attack is varied.

In figure 3 it may be noted that the lift-drag ratios of the three- and five-term solutions when operating at their design lift coefficients are considerably higher than the two-term solution of reference 1. It is also evident in figure 3 that the relative magnitude of the lift-drag ratios of the three sections decreases with increase in angle of attack. However, figure 3 shows that the reduction in L/D with increasing angle of attack is lessened by using higher values of $C_{L,d}$. Only the shaded

portion of figure 3 is considered of practical value because the hydrofoil must operate at finite angles of attack as will be pointed out in the following section.

APPROXIMATE LOCATION OF THE CAVITY BOUNDARY STREAMLINE

The desirability of operating as near the design lift coefficient as possible is obvious from figure 3. Therefore, since the hydrofoil must have some thickness, the minimum angle at which a hydrofoil with finite thickness can operate with a cavity from the leading edge is needed. The angle can be determined from the linearized theory of reference 1 by determining the location of the upper cavity boundary. The minimum angle at which the upper cavity streamline clears the upper surface of a hydrofoil of finite thickness is the angle desired. An approximate solution for the location of the cavity streamline is derived in the following analysis.

It is shown in reference 1 that the slope of the cavity upper surface formed on a two-dimensional hydrofoil operating at zero cavitation number and infinite depth can be obtained by transforming the vertical-velocity perturbations ahead of the equivalent airfoil to the cavity upper surface. These velocity perturbations are obtained by setting up the expression for the velocity induced at a point $-\bar{x}$, upstream of the equivalent airfoil. The procedure usually leads to very complex problems in integration, particularly if the series expansion of the vorticity distribution contributed by the camber is very lengthy. This complication is avoided in the analysis to follow by assuming that the vorticity contributed by the camber is concentrated at only one location, the center of pressure of the airfoil when $A_0 = 0$. The magnitude of the concentrated circulation is similarly prescribed. The method can be expected to give only an approximate answer, particularly if very much of the camber vorticity is located near the leading edge. However, for the new low-drag cambered sections being considered, the vorticity due to camber is in fact concentrated away from the leading edge (as indicated by fig. 2) and the approximation should be very good.

The hydrofoil and its equivalent transformed airfoil are shown in figure 4. The symbols used in figure 4 are those used in reference 1 where u and v are the velocity perturbations in the x- and y-directions in the hydrofoil plane, and $\bar{u}$ and $\bar{v}$ are the perturbations in the airfoil plane induced by the airfoil circulation. In the airfoil plane the vorticity is divided into two components

$$\Omega_\alpha = 2VA_0 \cot \frac{\theta}{2} \tag{51}$$

and

$$\Omega_c = 2V \sum_{n=1}^{k} A_n \sin n\theta \tag{52}$$

The first of these, Ω_α, is taken to be distributed over the chord exactly as given by equation (51). However, to simplify the problem, the second component of vorticity is assumed to be concentrated at one point on the chord - the center of pressure when $A_0 = 0$. This point is given in figure 4 as a distance $a\bar{c}$ aft of the leading edge. The magnitude of the concentrated vorticity is denoted as Γ_c (circulation due to camber) and is given by the following equation which is obtained from thin-airfoil theory (for example, see ref. 2):

$$\Gamma_c = \pi c V \frac{A_1}{2} \tag{53}$$

The velocities induced by the circulation contributed by A_0 are denoted as $\bar{v}_\alpha$, and those due to Γ_c are denoted as $\bar{v}_c$.

The slope of the cavity upper surface in the hydrofoil plane is

$$\frac{dy}{dx} = \frac{v(x)}{V} = \frac{\bar{v}(-\sqrt{x})}{V} = \frac{\bar{v}_\alpha(-\sqrt{x})}{V} + \frac{\bar{v}_c(-\sqrt{x})}{V} \tag{54}$$

and therefore

$$y = \int_0^x \frac{\bar{v}_\alpha(-\sqrt{x})}{V}\,dx + \int_0^x \frac{\bar{v}_c(-\sqrt{x})}{V}\,dx \tag{55}$$

The first term of equation (55) has been evaluated in reference 1; therefore, only the contribution due to camber need be considered here.

In figure 4 the induced velocity at any point along the $\bar{X}$-axis due to the circulation Γ_c is

$$\bar{v}_c(\bar{x}) = \frac{\pi\bar{c}V\frac{A_1}{2}}{2\pi\bar{c}\left(a - \frac{\bar{x}}{\bar{c}}\right)} = \frac{1}{4}\frac{A_1}{a - \frac{\bar{x}}{\bar{c}}}V \tag{56}$$

At a point forward of the airfoil $-\bar{x}$,

$$\bar{v}_c(-\bar{x}) = \bar{v}_c(-\sqrt{\bar{x}}) = \frac{1}{4}\frac{A_1}{a + \sqrt{\frac{x}{c}}}V \tag{57}$$

since $\bar{c} = \sqrt{c}$.

From equations (55) and (57)

$$\left(\frac{y}{c}\right)_c = \frac{A_1}{4c}\int_0^x \frac{1}{a + \sqrt{\frac{x}{c}}}\,dx = \frac{A_1}{2}\left[\sqrt{\frac{x}{c}} - a\log_e\left(\frac{a + \sqrt{\frac{x}{c}}}{a}\right)\right] \tag{58}$$

where the center of pressure of the airfoil a is found from the thin-airfoil theory, for $A_o = 0$, as

$$a = \frac{1}{2}\left(1 - \frac{1}{2}\frac{A_2}{A_1}\right) \tag{59}$$

By combining equation (58) with the linearized flat-plate solution of reference 1, the complete solution for the shape of the cavity upper streamline on arbitrary configurations is

$$y' = A_o\left[-x' + \frac{1}{2}\left(1 + 2\sqrt{x'}\right)\left(\sqrt{x' + \sqrt{x'}}\right) + \frac{1}{4}\log_e\left(1 + 2\sqrt{x'} - 2\sqrt{x' + \sqrt{x'}}\right)\right] + \frac{A_1}{2}\left[\sqrt{x'} - a\log_e\left(\frac{a + \sqrt{x'}}{a}\right)\right] \tag{60}$$

where x' and y' denote the dimensionless parameters, x/c and y/c. In this equation y is the distance from the X-axis to the cavity upper surface. When the hydrofoil reference line is at an angle of attack,

the actual distance l from the reference line to the cavity streamline is

$$\left.\begin{aligned} l &= y + \alpha x \\ \frac{l}{c} &= y' + \alpha x' \end{aligned}\right\} \quad \text{or} \quad (61)$$

as can be determined from figure 4. When equation (60) is substituted into equation (61) and A_0 is replaced by its equivalent $\alpha + A_0'$ from equation (8), the following equation is obtained:

$$\frac{l}{c} = A_0'x' + \left(\alpha + A_0'\right)\left[\frac{1}{2}\left(1 + 2\sqrt{x'}\right)\left(\sqrt{x' + \sqrt{x'}}\right) + \frac{1}{4}\log_e\left(1 + 2\sqrt{x'} - 2\sqrt{x' + \sqrt{x'}}\right)\right] + \frac{A_1}{2}\left[\sqrt{x'} - a\log_e\left(\frac{a + \sqrt{x'}}{a}\right)\right] \quad (62)$$

where l/c is the dimensionless-distance parameter from the hydrofoil reference line to the cavity upper surface.

By separating the angle of attack and camber contributions, equation (62) may be written as

$$\frac{l}{c} = \left(\frac{l}{c}\right)_\alpha + \left(\frac{l}{c}\right)_c = \left[\frac{\left(\frac{l}{c}\right)_\alpha}{\alpha}\right]\alpha + \left[\frac{\left(\frac{l}{c}\right)_c}{A_1}\right]A_1 \quad (63)$$

where for the case of $A_0' = 0$, which applies to the low-drag hydrofoils under consideration,

$$\frac{\left(\frac{l}{c}\right)_\alpha}{\alpha} = \frac{1}{2}\left(1 + 2\sqrt{x'}\right)\left(\sqrt{x' + \sqrt{x'}}\right) + \frac{1}{4}\log_e\left(1 + 2\sqrt{x'} - 2\sqrt{x' + \sqrt{x'}}\right)$$

and

$$\frac{\left(\frac{l}{c}\right)_c}{A_1} = \frac{1}{2}\left[\sqrt{x'} - a\log_e\left(\frac{a + \sqrt{x'}}{a}\right)\right]$$

For each low-drag hydrofoil, A_1 may be replaced by its equivalent in terms of $C_{L,d}$ and equation (62) may be written as

$$\frac{l}{c} = \left[\frac{\left(\frac{l}{c}\right)_\alpha}{\alpha}\right]\alpha + \left[\frac{\left(\frac{l}{c}\right)_c}{C_{L,d}}\right]C_{L,d} \tag{64}$$

where

$$\frac{\left(\frac{l}{c}\right)_c}{C_{L,d}} = K\left(\sqrt{x'} - a \log_e \frac{a + \sqrt{x'}}{a}\right)$$

and $K = \frac{A_1}{2C_{L,d}}$ which is $\frac{4}{5\pi}$ for the Tulin-Burkart design, $\frac{2}{3\pi}$ for the three-term design, and $\frac{3}{5\pi}$ for the five-term design.

The value of a may be determined from equation (59) and is 5/8, 3/4, and 5/6 for the Tulin-Burkart, three-term, and five-term hydrofoils, respectively. In figure 5(a), $\frac{\left(\frac{l}{c}\right)_\alpha}{\alpha}$ is plotted against x/c and in figure 5(b), $\frac{\left(\frac{l}{c}\right)_c}{C_{L,d}}$ is plotted against x/c for each of the low-drag hydrofoils. It is important to note the relative magnitudes of the coefficients $\frac{\left(\frac{l}{c}\right)_\alpha}{\alpha}$ and $\frac{\left(\frac{l}{c}\right)_c}{C_{L,d}}$ for a given value of x/c. At the trailing edge, $\frac{\left(\frac{l}{c}\right)_\alpha}{\alpha}$ is roughly 10 times as great as $\frac{\left(\frac{l}{c}\right)_c}{C_{L,d}}$. This means that except for small angles, the angle of attack is predominant in prescribing the cavity shape.

The adequacy of the assumption of concentrated camber vorticity is shown in figure 5(b) by comparing the solid (A) curve with the dashed one. The solid curve was computed from equation (58) and the dashed curve obtained from the coordinates given in reference 3. The tabulated coordinates of reference 3 were computed for the Tulin-Burkart section by considering the vorticity to be distributed as given in equation (52) and performing the necessary complicated integration.

In figure 6 the cavity shape derived from equation (64) for the low-drag hydrofoils is shown for $C_{L,d} = 0.2$. Also shown in figure 6 is the lower surface of each design for the value of $C_{L,d} = 0.2$. An interesting point (first noted in reference 3) is revealed in figure 6. The calculated cavity shape at the design angle of attack falls beneath the lower surface of the configuration. This result was not expected for these low-drag hydrofoils because the camber was selected to have positive pressure everywhere on the lower surface. It is believed that the disagreement is due to the inability of the linear theory to accurately predict the pressure distribution when the airfoil vorticity is not in reality distributed along the $\bar{X}$-axis. However, the shape of the cavity as determined from the linear theory is much less sensitive to the deviation of the true location of the vorticity from the $\bar{X}$-axis. That is, the distance from a point on the equivalent airfoil to a point forward of the leading edge is approximated very well by only the $\bar{x}$ component of the distance. Thus, it is seen that the pressure distribution predicted from the linear theory will be more nearly correct when the equivalent airfoil is at an angle of attack and more symmetrically located about the $\bar{X}$-axis. It appears, then, that low-drag hydrofoils such as those derived in the present paper and reference 1 can never be operated at the design angle of attack for the following two reasons: (1) an upper surface cavity will not form even on an infinitely thin configuration and (2) some thickness must be provided for strength. The possibility that, near the design angle of attack, the pressure distributions shown in figure 2 are incorrect has been indicated by experimental investigation in reference 4. Even at an angle of attack of 2°, cavitation was found to occur near the leading edge on the lower surface of the Tulin-Burkart configuration used in the investigation.

Because of the need for operating at finite angles of attack, the upper portion of figure 3 has been shaded to indicate that the lift-drag ratios calculated near the design lift coefficient are of academic interest only. In general, the minimum angle at which supercavitating flow from the leading edge is possible will be equal to or greater than about 2°. The exact minimum angle and, thus, the practical range of operation will be determined by the type and magnitude of camber and the thickness required for strength.

In figure 6 the cavity streamline shown may be considered as possible upper surfaces of practical hydrofoil configurations. For a given angle of attack the five-term hydrofoil permits a thicker leading edge and a more uniform section. These features are desirable structurally.

CONCLUSIONS

The principal results obtained in the application of the linearized theory to the design of new configurations may be summarized as follows:

1. The two-dimensional lift-drag ratios of the two new sections operating at their design lift coefficient are theoretically about 45 and 80 percent greater than the Tulin-Burkart configuration.

2. The relative magnitude of the lift-drag ratios of these new configurations as compared with those of the Tulin-Burkart design decrease with increase in angle of attack.

3. The simplified equation developed for the cavity boundary streamline for arbitrary shapes is in good agreement with the more exact solution for the Tulin-Burkart Section and should be adequate for all low-drag sections.

4. Low-drag hydrofoils developed from the linear theory cannot operate at the design angle of attack because an upper surface cavity will not form even for sections with zero thickness. The sections must be operated at an angle of attack slightly greater than the design angle.

Langley Aeronautical Laboratory,
National Advisory Committee for Aeronautics,
Langley Field, Va., July 2, 1957.

REFERENCES

1. Tulin, M. P., and Burkart, M. P.: Linearized Theory for Flows About Lifting Foils at Zero Cavitation Number. Rep. C-638, David W. Taylor Model Basin, Navy Dept., Feb. 1955.

2. Glauert, H.: The Elements of Aerofoil and Airscrew Theory. Second ed., Cambridge Univ. Press, 1947. (Reprinted 1948.)

3. Tachmindji, A. J., Morgan, W. B., Miller, M. L., and Hecker, R.: The Design and Performance of Supercavitating Propellers. Rep. C-807, David Taylor Model Basin, Navy Dept., Feb. 1957.

4. Ripken, John F.: Experimental Studies of a Hydrofoil Designed for Supercavitation. Project Rep. No. 52 (Contract N6onr-246 Task Order VI), Univ. of Minnesota, St. Anthony Falls Hydraulic Lab., Sept. 1956.

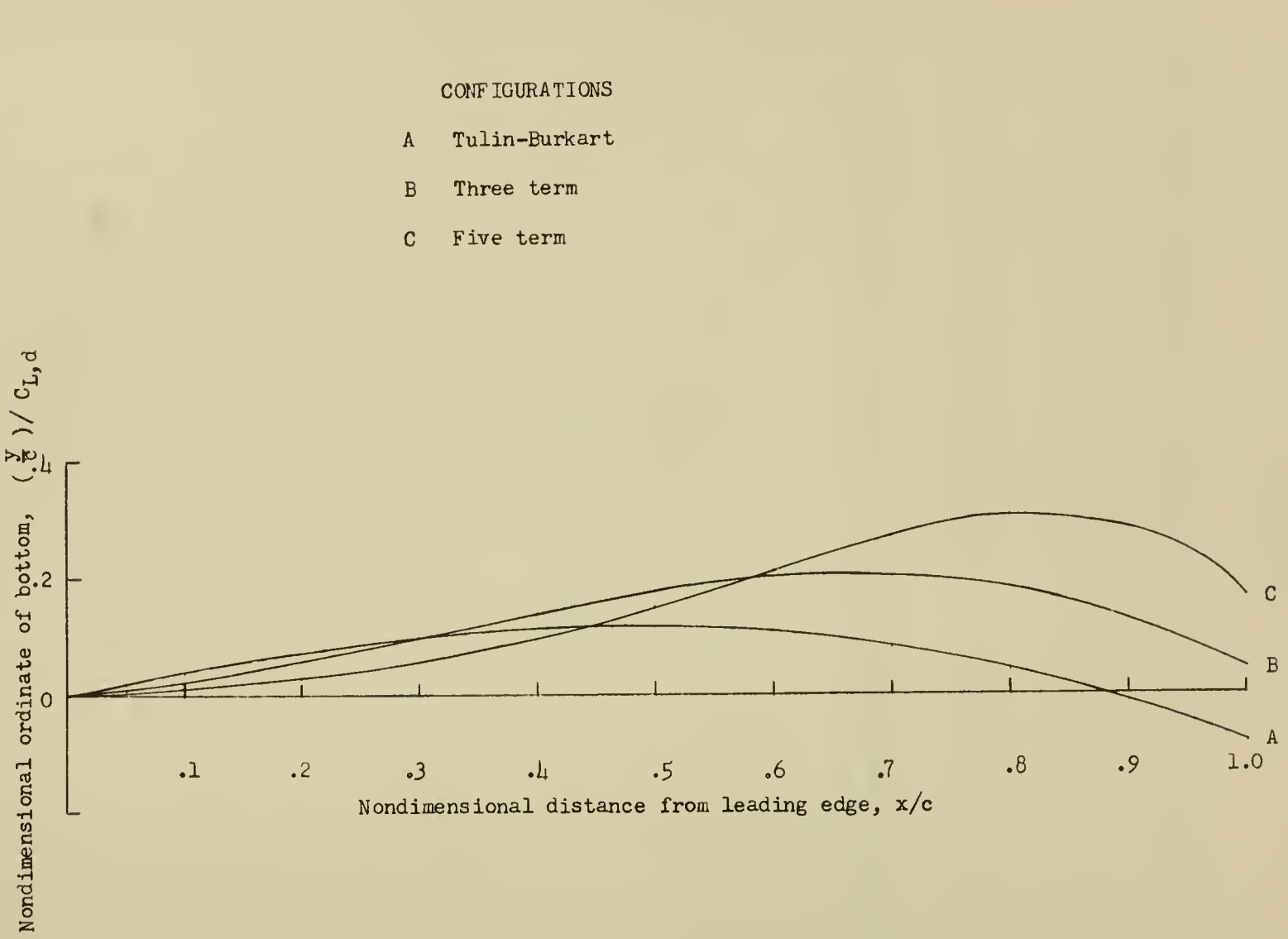

Figure 1.- Low-drag supercavitating hydrofoils. $\alpha = 0$.

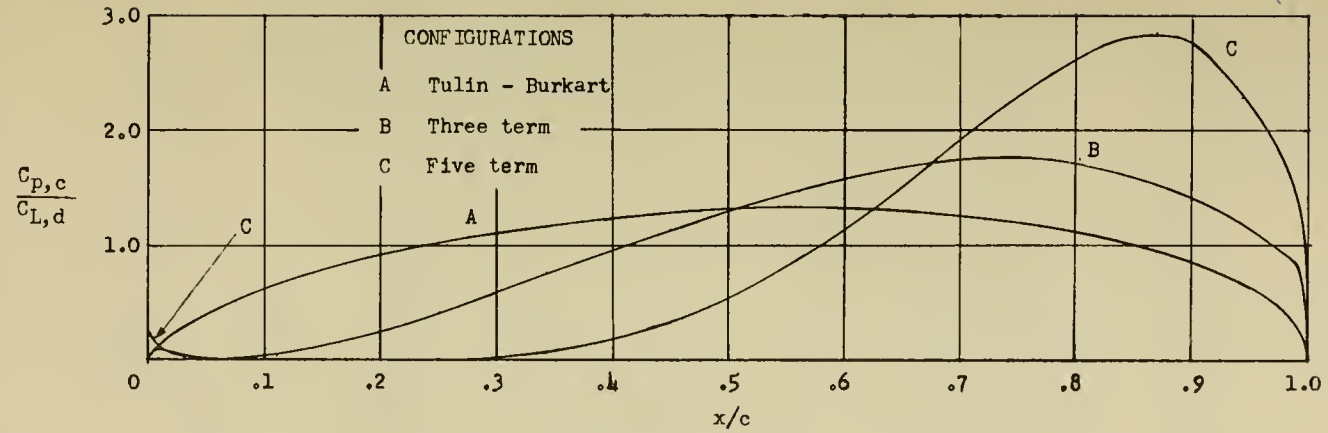

(a) Contribution due to camber.

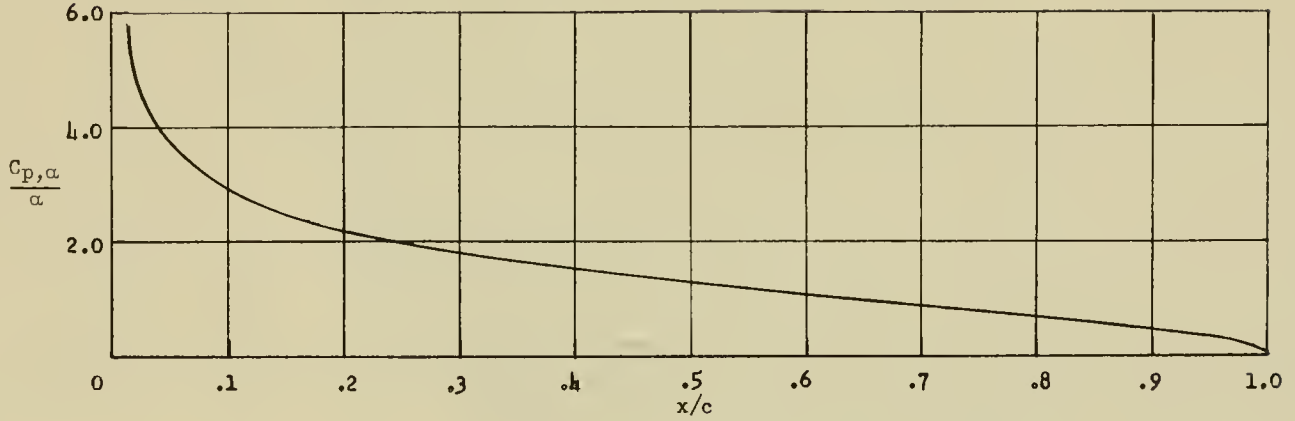

(b) Contribution due to angle of attack. $(C_p)_{total} = \left(C_p/C_{L,d}\right)C_{L,d} + \left(C_p/\alpha\right)\alpha$.

Figure 2.- Pressure distribution on low-drag supercavitating hydrofoils.

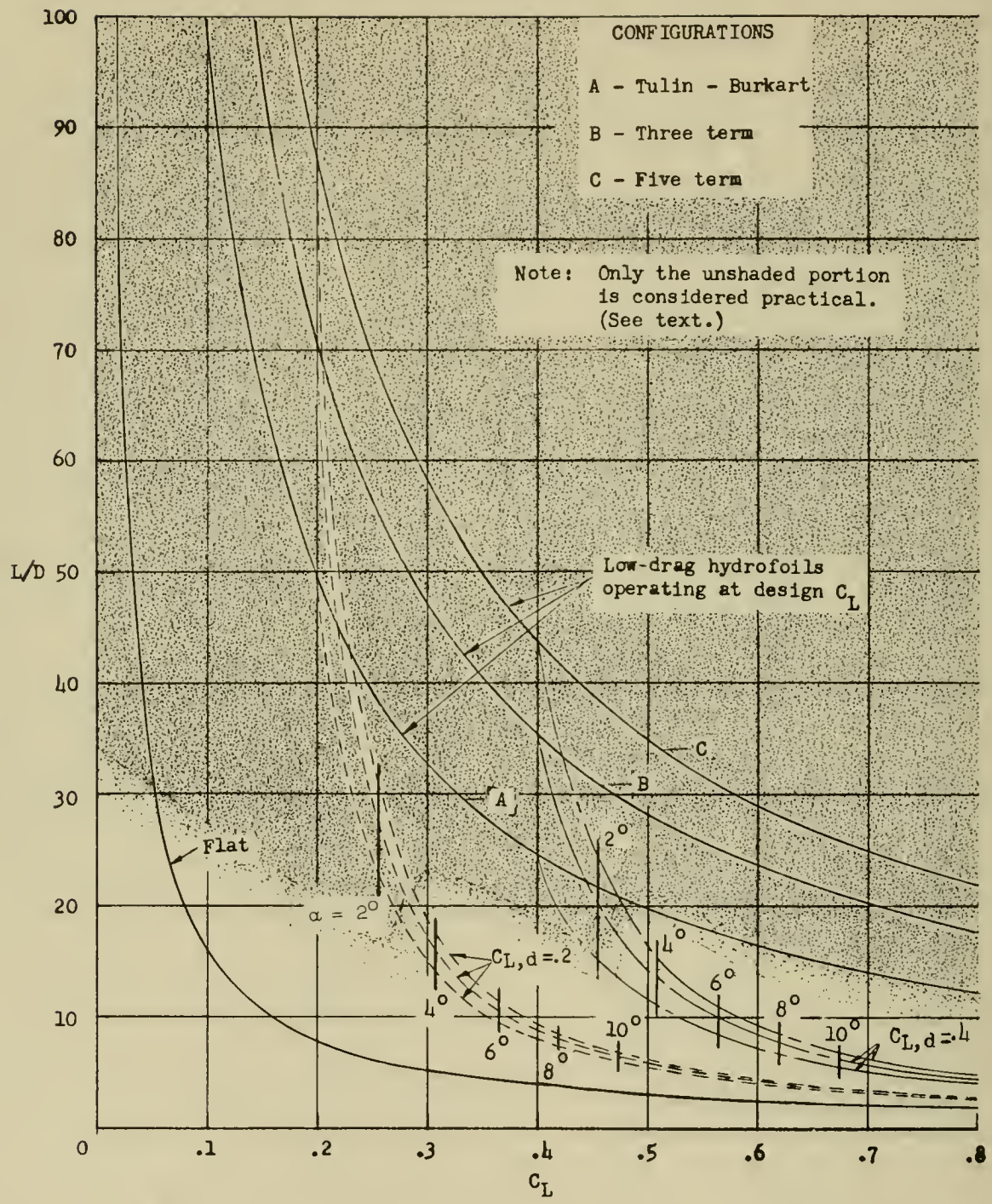

Figure 3.- Variation of L/D and C_L for low-drag hydrofoils.

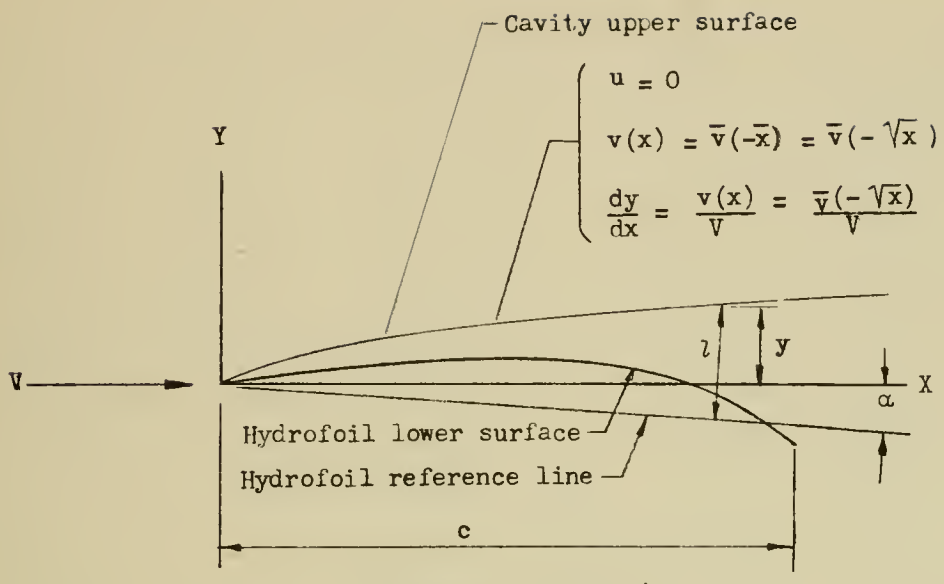

HYDROFOIL PLANE (Z)

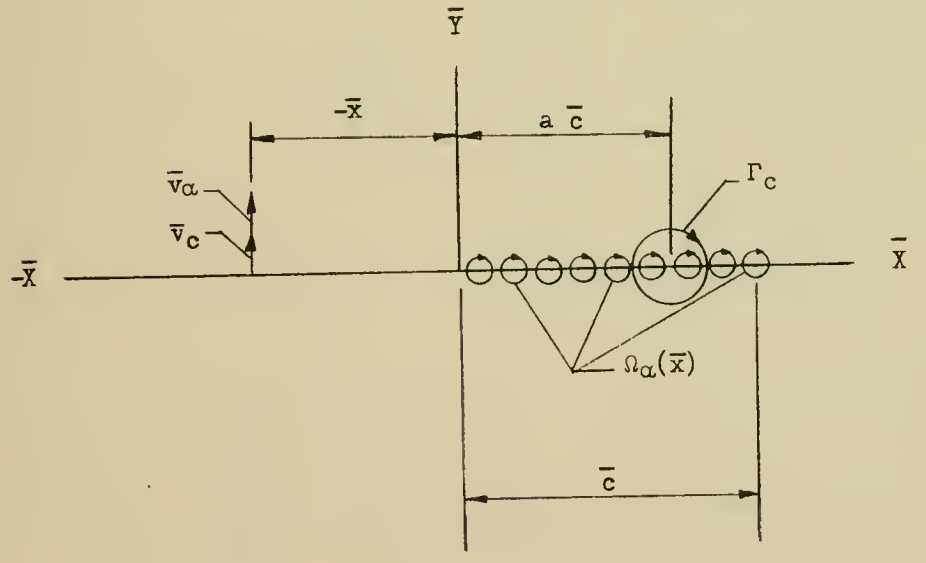

AIRFOIL PLANE ($\bar{Z} = -\sqrt{Z}$)

Figure 4.- The hydrofoil and equivalent airfoil planes.

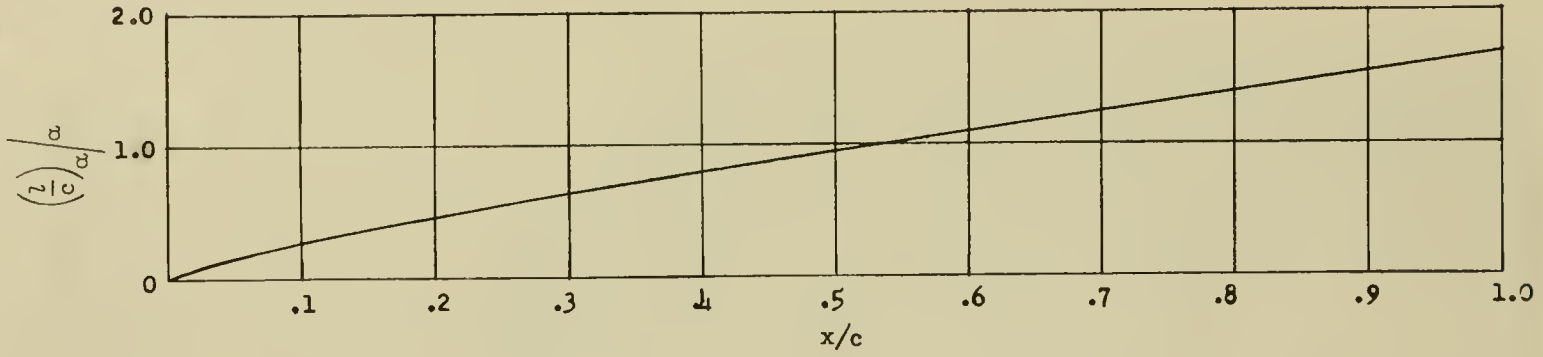

(a) Contribution due to angle of attack.

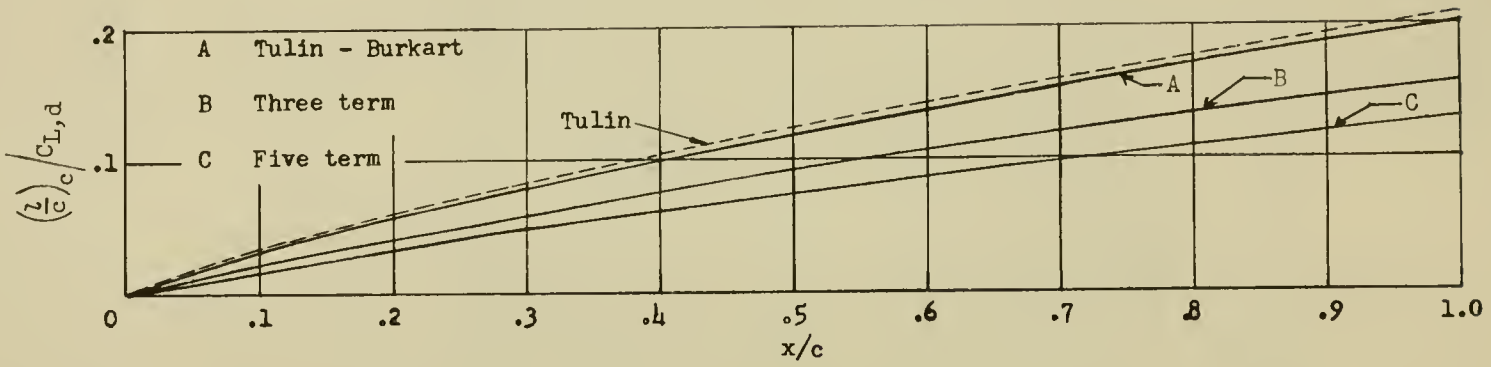

(b) Contribution due to camber. $\left(\frac{l}{c}\right)_{total} = \left[\left(\frac{l}{c}\right)_\alpha \Big/ \alpha\right]\alpha + \left[\left(\frac{l}{c}\right)_c \Big/ C_{L,d}\right] C_{L,d}$.

Figure 5.- Shape of the cavity upper surface.

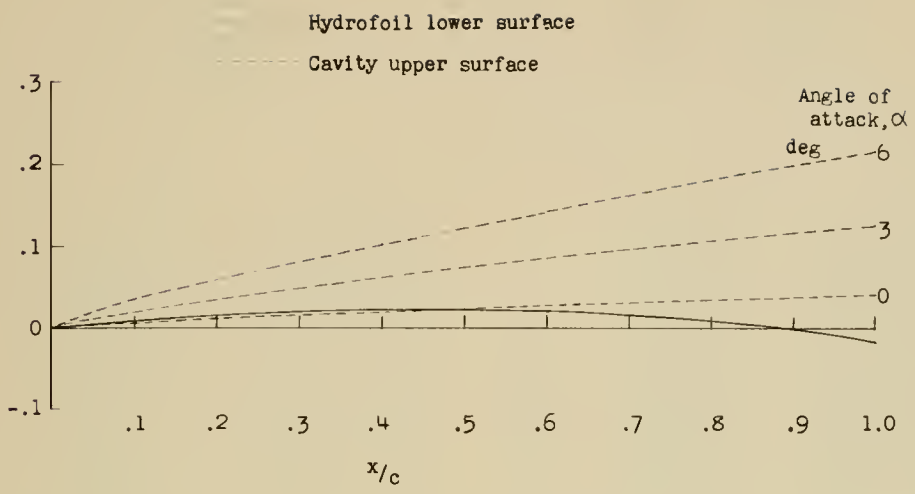

(a) Tulin-Burkart.

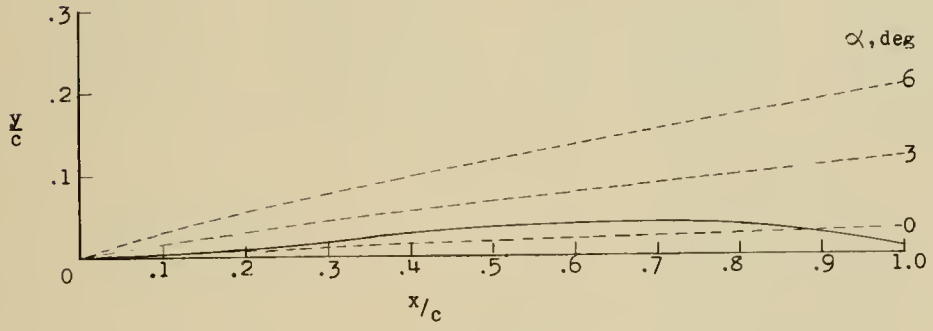

(b) Three term.

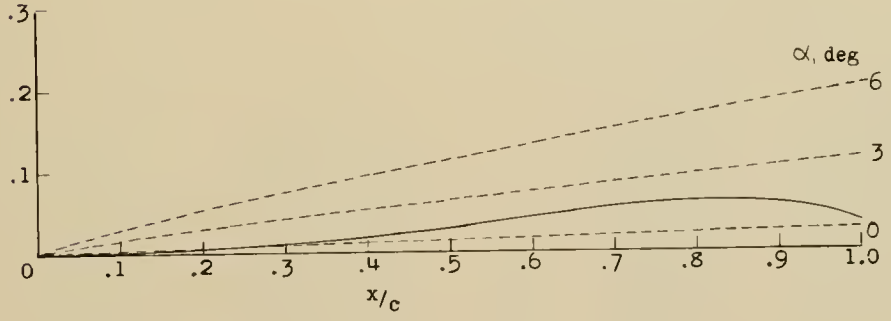

(c) Five term.

Figure 6.- Location of cavity upper surface for low-drag supercavitating hydrofoils, $C_{L,d} = 0.2$.

NACA RM L57G11a
National Advisory Committee for Aeronautics.
THEORETICAL DETERMINATION OF LOW-DRAG SUPERCAVITATING HYDROFOILS AND THEIR TWO-DIMENSIONAL CHARACTERISTICS AT ZERO CAVITATION NUMBER. Virgil E. Johnson, Jr. September 1957. 29p. diagrs. (NACA RM L57G11a)

Two new low-drag hydrofoils for operation at zero cavitation number are derived by the application of the Tulin-Burkart linearized theory. The two-dimensional lift-drag ratios of these two hydrofoils operating at design angle of attack are shown to be, theoretically, about 45 and 80 percent greater than the Tulin-Burkart configuration. A simplified calculation of the location of the upper cavity streamline for arbitrary configurations is also presented.

Copies obtainable from NACA, Washington

1. Wing-Section Theory (1.2.1.1)
2. Wing Sections - Camber (1.2.1.2.1)
3. Hydrodynamic Theory (2.1)
4. Hydrofoils (2.7)
I. Johnson, Virgil E., Jr.
II. NACA RM L57G11a

NACA

NACA RM L57G11a
National Advisory Committee for Aeronautics.
THEORETICAL DETERMINATION OF LOW-DRAG SUPERCAVITATING HYDROFOILS AND THEIR TWO-DIMENSIONAL CHARACTERISTICS AT ZERO CAVITATION NUMBER. Virgil E. Johnson, Jr. September 1957. 29p. diagrs. (NACA RM L57G11a)

Two new low-drag hydrofoils for operation at zero cavitation number are derived by the application of the Tulin-Burkart linearized theory. The two-dimensional lift-drag ratios of these two hydrofoils operating at design angle of attack are shown to be, theoretically, about 45 and 80 percent greater than the Tulin-Burkart configuration. A simplified calculation of the location of the upper cavity streamline for arbitrary configurations is also presented.

Copies obtainable from NACA, Washington

1. Wing-Section Theory (1.2.1.1)
2. Wing Sections - Camber (1.2.1.2.1)
3. Hydrodynamic Theory (2.1)
4. Hydrofoils (2.7)
I. Johnson, Virgil E., Jr.
II. NACA RM L57G11a

NACA

NACA RM L57G11a
National Advisory Committee for Aeronautics.
THEORETICAL DETERMINATION OF LOW-DRAG SUPERCAVITATING HYDROFOILS AND THEIR TWO-DIMENSIONAL CHARACTERISTICS AT ZERO CAVITATION NUMBER. Virgil E. Johnson, Jr. September 1957. 29p. diagrs. (NACA RM L57G11a)

Two new low-drag hydrofoils for operation at zero cavitation number are derived by the application of the Tulin-Burkart linearized theory. The two-dimensional lift-drag ratios of these two hydrofoils operating at design angle of attack are shown to be, theoretically, about 45 and 80 percent greater than the Tulin-Burkart configuration. A simplified calculation of the location of the upper cavity streamline for arbitrary configurations is also presented.

Copies obtainable from NACA, Washington

1. Wing-Section Theory (1.2.1.1)
2. Wing Sections - Camber (1.2.1.2.1)
3. Hydrodynamic Theory (2.1)
4. Hydrofoils (2.7)
I. Johnson, Virgil E., Jr.
II. NACA RM L57G11a

NACA

NACA RM L57G11a
National Advisory Committee for Aeronautics.
THEORETICAL DETERMINATION OF LOW-DRAG SUPERCAVITATING HYDROFOILS AND THEIR TWO-DIMENSIONAL CHARACTERISTICS AT ZERO CAVITATION NUMBER. Virgil E. Johnson, Jr. September 1957. 29p. diagrs. (NACA RM L57G11a)

Two new low-drag hydrofoils for operation at zero cavitation number are derived by the application of the Tulin-Burkart linearized theory. The two-dimensional lift-drag ratios of these two hydrofoils operating at design angle of attack are shown to be, theoretically, about 45 and 80 percent greater than the Tulin-Burkart configuration. A simplified calculation of the location of the upper cavity streamline for arbitrary configurations is also presented.

Copies obtainable from NACA, Washington

1. Wing-Section Theory (1.2.1.1)
2. Wing Sections - Camber (1.2.1.2.1)
3. Hydrodynamic Theory (2.1)
4. Hydrofoils (2.7)
I. Johnson, Virgil E., Jr.
II. NACA RM L57G11a

NACA

NACA RM L57G11a
National Advisory Committee for Aeronautics.
THEORETICAL DETERMINATION OF LOW-DRAG SUPERCAVITATING HYDROFOILS AND THEIR TWO-DIMENSIONAL CHARACTERISTICS AT ZERO CAVITATION NUMBER. Virgil E. Johnson, Jr. September 1957. 29p. diagrs. (NACA RM L57G11a)

Two new low-drag hydrofoils for operation at zero cavitation number are derived by the application of the Tulin-Burkart linearized theory. The two-dimensional lift-drag ratios of these two hydrofoils operating at design angle of attack are shown to be, theoretically, about 45 and 80 percent greater than the Tulin-Burkart configuration. A simplified calculation of the location of the upper cavity streamline for arbitrary configurations is also presented.

Copies obtainable from NACA, Washington

1. Wing-Section Theory (1.2.1.1)
2. Wing Sections - Camber (1.2.1.2.1)
3. Hydrodynamic Theory (2.1)
4. Hydrofoils (2.7)

I. Johnson, Virgil E., Jr.
II. NACA RM L57G11a

NACA RM L57G11a
National Advisory Committee for Aeronautics.
THEORETICAL DETERMINATION OF LOW-DRAG SUPERCAVITATING HYDROFOILS AND THEIR TWO-DIMENSIONAL CHARACTERISTICS AT ZERO CAVITATION NUMBER. Virgil E. Johnson, Jr. September 1957. 29p. diagrs. (NACA RM L57G11a)

Two new low-drag hydrofoils for operation at zero cavitation number are derived by the application of the Tulin-Burkart linearized theory. The two-dimensional lift-drag ratios of these two hydrofoils operating at design angle of attack are shown to be, theoretically, about 45 and 80 percent greater than the Tulin-Burkart configuration. A simplified calculation of the location of the upper cavity streamline for arbitrary configurations is also presented.

Copies obtainable from NACA, Washington

1. Wing-Section Theory (I.2.1.1)
2. Wing Sections - Camber (1.2.1.2.1)
3. Hydrodynamic Theory (2.1)
4. Hydrofoils (2.7)

I. Johnson, Virgil E., Jr.
II. NACA RM L57G11a

NACA RM L57G11a
National Advisory Committee for Aeronautics.
THEORETICAL DETERMINATION OF LOW-DRAG SUPERCAVITATING HYDROFOILS AND THEIR TWO-DIMENSIONAL CHARACTERISTICS AT ZERO CAVITATION NUMBER. Virgil E. Johnson, Jr. September 1957. 29p. diagrs. (NACA RM L57G11a)

Two new low-drag hydrofoils for operation at zero cavitation number are derived by the application of the Tulin-Burkart linearized theory. The two-dimensional lift-drag ratios of these two hydrofoils operating at design angle of attack are shown to be, theoretically, about 45 and 80 percent greater than the Tulin-Burkart configuration. A simplified calculation of the location of the upper cavity streamline for arbitrary configurations is also presented.

Copies obtainable from NACA, Washington

1. Wing-Section Theory (I.2.1.1)
2. Wing Sections - Camber (1.2.1.2.1)
3. Hydrodynamic Theory (2.1)
4. Hydrofoils (2.7)

I. Johnson, Virgil E., Jr.
II. NACA RM L57G11a